Ocean Sci. Discuss., https://doi.org/10.5194/os-2017-93
Manuscript under review for journal Ocean Sci.
Discussion started: 15 January 2018

Ocean Science
Discussions
Open Access
EGU

Mesoscale Eddies in the Algerian Basin: do they differ as a function of their formation site?

Federica Pessini[1], Antonio Olita[1], Yuri Cotroneo[2], and Angelo Perilli[1]

[1]IAMC CNR di Oristano, Oristano, Italy
[2]Università degli Studi di Napoli "Parthenope", Napoli, Italy

Correspondence to: Federica Pessini (federica.pessini@iamc.cnr.it)

Abstract. The circulation of the Western Mediterranean Sea (WMED) is dominated by highly variable and heterogeneous mesoscale circulation, strongly driven by the formation and propagation of eddies (cyclonic and anticyclonic) mainly acting in the Algerian Basin. Anticyclones are characterized by longer life, so potentially contributing to a large extent to the mesoscale characterization of the basin. Hereafter we will take into account only anticyclonic structures.

In order to investigate the spatial and temporal distribution of eddy generation and their respective paths in the Algerian Basin, the most energetic WMED portion, we use an automated detection and tracking hybrid method (modified to fill the gaps in single eddy tracks) applied to 22 years of Sea Level Anomaly (SLA) data. The method is based on the computation of the Okubo-Weiss parameter in SLA closed loops.

We find that anticyclonic short-life eddies mostly occur in the northern portion of the domain, north of 39° N, along the North Balearic Front (NBF). We refer to all the structures formed in that area as Frontal Anticyclonic Eddies (FAEs). Such short-life eddies are characterized by low translational velocity and a highly variable direction of propagation. We found a weak seasonality in their formation, with maxima in fall and winter. By contrast, anticyclonic longer-life eddies tend to arise in the southern part of the basin, along the Algerian Current, with a clear maximum in spring. All the structures originating along the Algerian Current are known as Algerian Eddies (AEs).

According to previous studies, we observe that AEs mainly form east of 6.5° E and move eastward along the African coast to the Sardinia Channel, where they detach from the coast, continuing offshore and following the cyclonic intermediate circulation. We detect a region where such eddies tend to converge and terminate their life.

Finally, the analysis suggests that the Algerian Basin can be separated in two parts, southern and northern one as function of the eddy properties like formation site, path, number, energy and lifetime. The only connection in terms of eddy tracks between the two areas is represented by a few FAEs moving southward and being entrapped in the southern cyclonic circulation.

1 Introduction

The Algerian Basin, located in the southern part of the Western Mediterranean Sea (WMED) and here defined as the area of the Mediterranean Sea between the African coast, the Balearic Islands and Sardinia, is quite a small basin, characterized by both large scale and mesoscale dynamics as also shown in Figure 1, where the Mean Dynamic Topography (MDT) from Rio

Ocean Sci. Discuss., https://doi.org/10.5194/os-2017-93
Manuscript under review for journal Ocean Sci.
Discussion started: 15 January 2018

et al. (2014) is reported. The MDT is the permanent stationary component of the ocean dynamic topography and efficiently represents the main circulation of the basin. The Atlantic Water (AW) flowing from the Gibraltar Strait follows eastward along the Algerian slope and forms the Algerian Current (AC). Past the Greenwich Meridian, the current becomes shallower and wider near the Sardinia Channel (Millot, 1985; Fusco et al., 2008; Budillon et al., 2009). Mainly because of the difference in density between AW and the Mediterranean surrounding water (MW), this along-slope current frequently becomes unstable and meanders, generating mesoscale eddies as a result of baroclinic instabilities (Obaton et al., 2000). These structures can be both cyclonic and anticyclonic, but the former are limited to the upper layer and short-lived and do not affect significantly the mean circulation of the basin. Hereafter, for the purposes of the present study, we will consider only the Algerian anticyclonic Eddies, indicated with the acronym AEs. The general description of their behaviour, as reported in the bibliography, is that they move along the African coast at a few Km per day and are blocked at the level of the Sardinia Channel (Millot, 1985, 1999; Font et al., 1998, 2004; Olita et al., 2011), where they are usually forced by the local topography to detach from the coast and follow a cyclonic pathway (Millot, 1987; Vignudelli, 1997; Cotroneo et al., 2016; Aulicino et al., 2018).

Mesoscale eddies in the Mediterranean sea have been widely investigated in the past (Burkov et al., 1979) with in situ data (Benzhora and Millot, 1995a; Millot, 1999), moorings, surface drifters (Font et al., 2004), altimetry observations (Isern-Fontanet et al., 2005; Escudier et al., 2016; Mason and Pascual, 2013; Mason et al., 2014) and numerical models (Levy et al., 1999, 2000). Most data on the motion of the eddies are provided by infrared and colour satellite imagery (Millot, 1985), as their cores are warmer than the surrounding water except in winter, when the gradient tends towards zero or inverts (Puillat et al., 2002). The biological response associated with eddies is remarkable and is usually highlighted by ocean colour signatures that could be used as a tracer (Moràn et al., 2001; Taupier-Letage et al., 2003; Olita et al., 2014). The limit of this survey technique is the cloud cover, which does not allow continuous data recording, especially during winter. To avoid the limitations associated with infrared and colour satellite imagery, mesoscale phenomena can be investigated with altimetry observations, such as Absolute Dynamic Topography (ADT) and Sea Level Anomaly (SLA). They are not affected by cloud cover and provide the geostrophic velocity field, but with coarser spatial resolution than infrared and optical passive sensors.

The complexity of the dynamics in the Algerian Basin and its influence on the circulation of the entire WMED stimulated the study of these structures and their motion. Puillat et al. (2002) analysed a long dataset of Sea Surface Temperature (SST) and observed AEs with lifespan up to 3 years. Henceforth, several automated detection and tracking algorithms applied to altimetry data have been developed. An analysis of Escudier et al. (2016) based on SLA data in the Mediterranean reveals three preferred areas of formation for the AEs and also provides their mean pathways. In particular, structures formed between 6° E and 7° E remain for a long time close to the area of formation or detach from the coast, following the large-scale cyclonic Algerian Gyre (AG). These features form most commonly during specific seasons and have significant inter-annual variability over the last 20 years.

In literature, other eddies of the Algerian Basin with different origins are described and labelled with several names, mainly as function of the formation area (more than on intrinsic eddy characteristics). Testor et al. (2005a) named Sardinian Eddies (SEs) the structures associated with the detachment from the continental slope of Sardinia of the AG. Contrary to AEs, which are baroclinic, these features are described by the Authors as strongly barotropic with a typical radius of about 30 Km. They

also present a marked core of Levantine Intermediate Water (LIW) with high temperature at intermediate depths. The values of salinity and temperature of this core are similar to those found in the LIW vein along the Sardinian coast. SEs show a clear surface signature months after the detachment from the coast of Sardinia and their lifespan is of the order of several months.

The cyclonic mean circulation of the Algerian Basin is separated from the cyclonic mean circulation of the northern Provençal Basin by the North Balearic Front (NBF), a thermal front characterized by a high seasonal variability (Ruiz et al., 2009; Olita et al., 2011). Typically, AW entering through the Strait of Gibraltar flows eastward at the Algerian Basin surface, while MW formed in the eastern and northern parts of the Mediterranean flows westward at the intermediate and deep layers (Millot, 1985; Aulicino et al., 2018). The surface layer presents large variability, while the deepest layers (below the LIW) are relatively uniform (Budillon et al., 2009) but could experience long term changes, as observed in Fusco et al. (2008). An averaged west-east current, the Western Mid-Mediterranean Current (WMMC) (Pinardi et al., 2013), flows eastward from the Balearic Islands to the west coast of Sardinia in correspondence with the NBF. The front is affected by the seasonality of the north-westerly winds and reaches its southernmost position in winter. Along the current, baroclinic instabilities occur, probably contributing to the generation of meanders and eddies. From in situ data and satellite data sets Fuda et al. (2000) observed several eddies propagating westward at a few Km/day along the NBF and named them Frontal Anticyclonic Eddies (FAEs). They are short-lived and they usually present signature of Winter Intermediate Water (WIW) and LIW.

In spite of the current body of research, a comprehensive study of the tracking, energy and interaction of all kind of eddies forming and acting in the Algerian Basin is still lacking. In particular, the differences occurring among the eddies of different origin are still not completely known, as the analysis of Escudier et al. (2016) focused just on the AEs (neglecting in its analysis eddies formed outside the Algerian Current).

Our study aims to shed light on the different statistical characteristics (energy, path, formation areas, lifetime, etc.) of the two main types of Anticyclonic eddies (AEs and FAEs) in the Algerian Basin. This was done through a series of eulerian statistics (performed on a regular grid) computed on the output of the lagrangian tracking method adopted. The automated detection and tracking method used is a hybrid method (combination of the physical and the geometrical approaches) performed by Penven and Echevin (2005) and Halo et al. (2014), and it is detailed in the following section. Such method was applied on a long-term time series (22 years) of daily SLA fields, so providing a robust basis for statistical analysis.

Dataset, detection and tracking method are described in depth in Section 2. The results of our study are presented in Section 3. At first, we plotted the distribution of the eddies in the basin and their relative vorticity. Then we observed the distribution in time of the mean kinetic energy and its relation with the eddy lifetimes. We further computed separate eulerian statistics of the formations and terminations of the structures for both short-life and long-life eddies. Lastly, we observed the trajectories of the eddies and plotted the tracks and their translational velocity. In section 4 we summarize and discuss the results, and take our conclusions.

Ocean Sci. Discuss., https://doi.org/10.5194/os-2017-93
Manuscript under review for journal Ocean Sci.
Discussion started: 15 January 2018

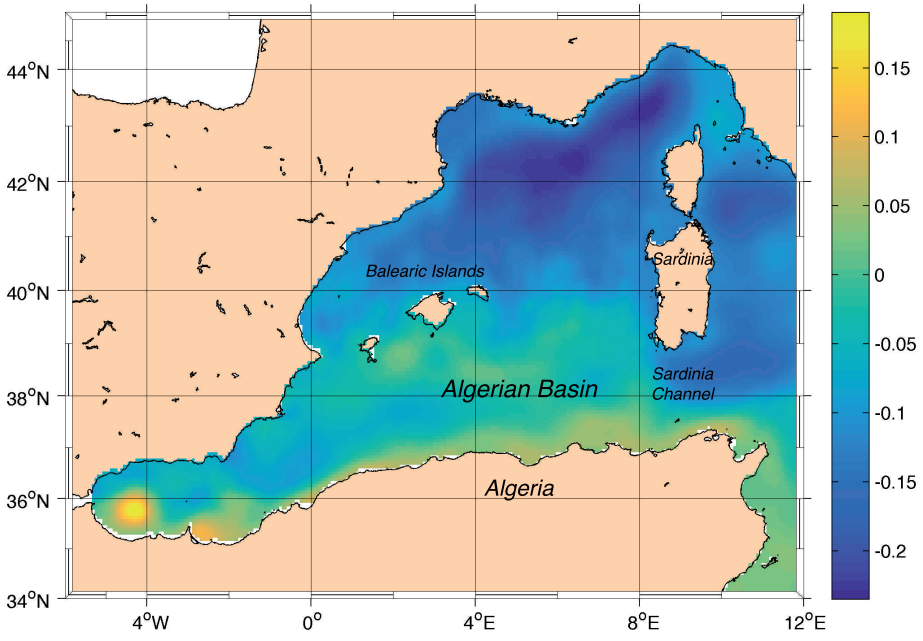

Figure 1. Mean Dynamic Topography (m) in the WMED. (Rio et al., 2014).

2 Materials and methods

Eddy detection and tracking algorithms based on altimetry data have been widely used to investigate mesoscale structures in both space and time (Isern-Fontanet and E. Garcìa-Ladona, 2003; Chelton et al., 2007, 2011; Escudier et al., 2016; Yi et al., 2014; Schütte et al., 2016; Mason and Pascual, 2013). These algorithms, applied on global and regional scales, have been successful in the characterization of several properties, such as polarity, propagation pathway, lifetime, radius and amplitude. They can be applied to altimetry data sets or with realistic high-resolution numerical model outputs, which also offer the opportunity to study both surface and subsurface eddies, as well as three-dimensional structures. Several comparisons have been done with both data sets and literature (Chelton et al., 2011; Kurian et al., 2011).

Many different methods have been developed for detecting eddies, but in general they fall into two main categories: physical and geometrical methods. The former are based on the calculation of some dynamic fields and define eddies based on the closed contours of a threshold value. The physical fields computed are SLA, Sea Surface Height (SSH) (Chelton et al., 2011; Chaigneau et al., 2009), vorticity (McWilliams, 1999) and velocity gradient tensor or Okubo-Weiss parameter (W) (Penven and Echevin, 2005; Chelton et al., 2007; Isern-Fontanet and E. Garcìa-Ladona, 2003). On the other hand, geometrical methods

Ocean Sci. Discuss., https://doi.org/10.5194/os-2017-93
Manuscript under review for journal Ocean Sci.
Discussion started: 15 January 2018

are based on the curvature or shape of the instantaneous flow field. Several studies make use of both physical and geometrical methods to better explain the structure of mesoscale eddies.

In this work we used the SLA closed contour method combined with the Okubo-Weiss parameter (hybrid method), which remains the most popular technique due to its simplicity and computational efficiency. After the detection, the tracking algorithm identified the trajectories of the eddies and extrapolated several properties. In the next sections we describe the automated method of detection and tracking and the modifications we introduced to improve the results.

The altimetry data used are the merged, delayed-time gridded maps of optimally interpolated SLA, previously available courtesy of Archiving, Validation and Interpolation of Satellite Oceanographic (AVISO) and now distributed by Copernicus Marine Environment Monitoring Service (CMEMS). These data are produced by the SL-TAC multi-mission altimeter data processing system. The *all-sat* gridded SLA fields consider all available altimeters and therefore have higher quality levels, although not homogeneous in time due to the time-varying mission configuration. The horizontal resolution of the data is $1/8°$ (about 14 Km) and data are available from January 1993.

Details on the data, products and processing procedures are available on the SSALTO/DUACS User Handbook www.aviso.altimetry.fr/fileadmin/documents/data/duacs/Duacs2014.pdf.

In order to explain step by step the adopted hybrid method, we firstly describe in detail the Okubo-Weiss-based detection methods (Section 2.1). Then, we details the changes adopted to obtain the hybrid method highlighting its pros and cons.

2.1 The Okubo-Weiss-based detection method

The Okubo-Weiss-based detection methods permit the separation of the cores of the eddies from the surrounding water on the basis of their physical properties.

The Okubo-Weiss parameter W is defined as follows:

$$W = \sigma_n^2 + \sigma_s^2 - \omega^2, \tag{1}$$

where σ_n, σ_s are the normal and the shear components of the strain and ω is the relative vorticity of the flow and they are expressed as:

$$\sigma_n^2 = \frac{\partial u}{\partial x} - \frac{\partial v}{\partial y} \tag{2}$$

$$\sigma_s^2 = \frac{\partial v}{\partial x} + \frac{\partial u}{\partial y} \tag{3}$$

$$\omega = \frac{\partial v}{\partial x} - \frac{\partial u}{\partial y}. \tag{4}$$

This method has proved its efficiency in separating the eddy core from the circulation cell in terms of the sign of the Okubo-Weiss parameter (Jeong and Hussain, 1995; Pasquero and A. Provenzale, 2001; Isern-Fontanet and E. Garcìa-Ladona, 2003). Negative values of W correspond to the inner part of the eddy, the vorticity-dominated region, while positive values indicate the external part, dominated by strain. The borders of the structures are characterised by $W = 0$ (Chelton et al., 2007), while the areas of the structures found by this method correspond to the closed loops of the parameter W, which present negative

Ocean Sci. Discuss., https://doi.org/10.5194/os-2017-93
Manuscript under review for journal Ocean Sci.
Discussion started: 15 January 2018

values. The physical method has advantages and disadvantages, discussed in Section (2.6). In the next section we describe the hybrid method.

2.2 The hybrid detection method

In this work we used a hybrid detection method (Halo et al., 2014): a combination of detecting the largest contours in SLA data (geometric criteria (Chelton et al., 2011)) and computing the W parameter (traditional physical method (Chelton et al., 2007)). The number of tunable parameters is thus reduced to three. Some tests have demonstrated that the number of detected eddies does not change appreciably by varying them (Halo et al., 2014).

The eddy detection and tracking routines are coded in MatLab and are freely available for download at https://sourceforge.net/projects/eddydetect/ thanks to Pierrick Penven. We adapted the algorithm to our area of study, introducing some modifications and tuning the parameters. The algorithm has evolved thanks to many tests and was calibrated by comparison with independent satellite imagery (ocean color and infrared, not shown).

The code can be divided in two main parts: the eulerian one, dedicated to the detection of the eddies (eddy detection), and the lagrangian one, which investigates their trajectories (eddy tracking).

The eulerian part concerns eddy detection starting from SLA data. After selecting a domain and a period of time the algorithm looks for the nearest dates of data available, then identifies the local maxima and minima that could eventually correspond to anticyclonic and cyclonic eddies respectively. Then W is computed starting from geostrophic velocities. In order to reduce the grid scale noise, 2 passes of a Hanning filter are applied. The largest closed contours of negative W inside the SLA closed loops are considered to be an eddy. The closed loops of W are the border of the structures and correspond to the separation between the vorticity-dominated and the deformation-dominated region.

The following list summarises the main steps of the code:

- Selection of the spatial and temporal range to analyse.
- Selection of the interval between the SLA contours, which should approximate the precision of the altimetry. We choose 0.02 m.
- An upper threshold for Okubo-Weiss parameter detection is fixed at 0.
- A minimum value for SLA is fixed at 0.
- Selection of the number of Hanning filter iterations on the Okubo-Weiss parameter. We choose 2 passes.
- The algorithm finds the local extrema in SLA.
- The algorithm computes the geostrophic rotational velocities, the W parameter, the vorticity and the Eddy Kinetic Energy (EKE).
- If the W parameter is negative within a closed loop of SLA, the algorithm computes the number of grid points inside the eddy. If this number is greater than 4, the detected structure can be considered a mesoscale eddy.

Ocean Sci. Discuss., https://doi.org/10.5194/os-2017-93
Manuscript under review for journal Ocean Sci.
Discussion started: 15 January 2018

– The algorithm checks if there are other extrema in this eddy, with negative W. In this case the algorithm detects more separated structures.

– The code extrapolates all the properties of the eddy such as position, time, area, surface kinetic energy, vorticity, equivalent radius (computed from the area), maximum, minimum and mean sea surface height (SLA), amplitude, rotational speed (Chelton et al., 2011) and finally zonal and meridional propagation velocities.

– After the detection step, a routine selects the eddies with radius included in the range $0 - 300$ Km and amplitude greater than zero m (tunable parameters). A new file with all the properties computed is written in this phase. It will be used later by the lagrangian routines in order to track the eddies.

The hybrid method has been applied over the period from January 1993 to December 2014 to the domain between 2° E and 10° E and from 37° N to 42° N.

2.3 Parameters of the eddies

Once the structures are defined, the kinetic energy of each point of the eddy is calculated. The kinetic energy has been computed starting from the geostrophic velocities. Throughout we will refer to the kinetic energy normalized by mass.
The total areal kinetic energy (*AEKE*) is defined as follows:

$$AEKE = \sum_{k=1}^{N} EKE_k ds_k \tag{5}$$

where EKE_k (cm^2/s^2) and ds_k (cm^2) are respectively the kinetic energy and the unit of area for each point of the grid inside the eddy. N is the number of unit of area inside the eddy.
The area of the eddy S (cm^2) is:

$$S = \sum_{k=1}^{N} ds_k. \tag{6}$$

The *EKE* (cm^2/s^2) is the energy of each eddy centre, calculated as:

$$EKE = \frac{AEKE}{S}, \tag{7}$$

The total daily EKE ($tdEKE$) is the sum of the EKEs of all the eddy centres for each day:

$$tdEKE = \sum_{i=1}^{n\,eddies} EKE_i \tag{8}$$

where $n\,eddies$ is the number of the eddies of each day. It is measured in cm^2/s^2.
The monthly mean EKE (cm^2/s^2) is calculated as:

$$mmEKE = \frac{1}{T} \sum_{d=1}^{T} tdEKE_d \tag{9}$$

Ocean Sci. Discuss., https://doi.org/10.5194/os-2017-93
Manuscript under review for journal Ocean Sci.
Discussion started: 15 January 2018

where T is the number of the days for each month.

The other parameters are calculated as follows:

- The coordinates of the eddy centres are the coordinates of the geometric centre of the closed contour:

$$Longitude = \frac{\sum_{k=1}^{N} lon_k}{N}, \tag{10}$$

$$Latitude = \frac{\sum_{k=1}^{N} lat_k}{N}; \tag{11}$$

- The vorticity ξ of the centres as:

$$\xi = \frac{\sum_{k=1}^{N} \xi_k \, ds_k}{S} \tag{12}$$

where ξ_k is the vorticity of each point of the grid inside the eddy.

- Radius (m):

$$R = \sqrt{\frac{S}{\pi}} \tag{13}$$

- Amplitude (m):

$$A = max(h) - min(h), \tag{14}$$

where h is the SLA value for the eddy, in m. It is defined as the difference between the estimated basal height of the eddy boundary and the extremum value of SLA within the eddy interior.

After having detected the structures over the daily maps of SLA data we applied the tracking algorithm to identify the trajectories of each eddy. The tracking method is described in the next section.

2.4 The tracking algorithm

The second part of the code is the lagrangian one, which provides information about the lifetime of the eddies and of their trajectories.

Penven and Echevin (2005) proposed a method to track the eddies based on a generalized distance. After having selected the structures with correct properties, the algorithm detects an eddy in one frame and checks its presence in the subsequent frame, comparing each eddy with the structures of the following day. It takes into account the difference in coordinates, radius, vorticity, mean height and amplitude between two successive days. For each eddy e_1 of the initial day and for each eddy e_2 of the following day, X_{e_1,e_2} is defined as a general distance in a non-dimensional property space:

$$X_{e_1,e_2} = \left[\left(\frac{L}{L_0} \right)^2 + \left(\frac{R_2 - R_1}{R_0} \right)^2 + \left(\frac{\xi_2 - \xi_1}{\xi_0} \right)^2 + \left(\frac{SLA_{mean_2} - SLA_{mean_1}}{Z_0} \right)^2 + \left(\frac{Amp_2 - Amp_1}{A_0} \right)^2 \right]^{\frac{1}{2}} \tag{15}$$

Ocean Sci. Discuss., https://doi.org/10.5194/os-2017-93
Manuscript under review for journal Ocean Sci.
Discussion started: 15 January 2018

where L is the spherical distance between the eddies and $R_2, R_1, \xi_2, \xi_1, SLA_{mean_2}, SLA_{mean_1}, Amp_2, Amp_1$ are respectively the radius, the vorticity, mean SLA variations and amplitude of e_2 and of e_1. The typical values, according to the dimension and to the properties of the Algerian Basin, are listed below:

- $L_0 = 80$ Km is the typical eddy distance ;
- $R_0 = 70$ Km is the typical eddy radius scale;
- $\xi_0 = 10^{-5}\ s^{-1}$is the typical eddy vorticity scale;
- $Z_0 = 0.1$ m is the typical eddy mean SLA variations;
- $A_0 = 0.1$ m is the typical eddy SLA amplitudes variation.

The eddy pair which minimises the general distance is considered to be the same eddy evolving in time in all cases, except when the two following conditions are satisfied simultaneously: the eddy speed is greater than $U_{max} = 0.3$ m/s and the distance between the two structures (L_0) is greater than twice the radius of the first eddy ($> 2R_1$).

The algorithm counts an eddy each day when it is detected on a map of SLA and assigns an ID to facilitate the extrapolation of their properties. Eddies with the same ID are the same eddy evolving over time (eddy tracking). The method ensures that an eddy preserves its polarity, that is, a cyclonic or anticyclonic structure. No cyclones become anticyclones, and the translational speed remains in a realistic range of a few kilometres per day. If an eddy travels at an unrealistic translational speed, it is considered as a different eddy with a new ID.

We calculated for each eddy the date of formation, the date of termination, the lifetime, the translational velocity and the mean kinetic energy.

We refer to the mean kinetic energy ($MEKE$) of each eddy with the formula:

$$MEKE = \frac{\sum_{d=1}^{lt} EKE_d}{lt}, \tag{16}$$

where the lt is the lifetime in days and the MEKE in cm^2/s^2.

2.5 Detection algorithm changes

The altimetry presents many difficulties to fully resolve the mesoscale activity in the Algerian Basin because of the small eddy radii and the resolution limitations of altimetry data. The structures moving across the basin occasionally encounter other structures and can deviate from their pathway, lose intensity or merge in a new stronger eddy (coalescence). These different behaviours are not always recognised by the algorithm, which can mistakenly assume the termination of an eddy and the formation of a new one. In fact, the daily SLA data are the results of the interpolation of several satellites in different and complementary temporal ranges. As a consequence, any weak signal in vorticity could be lost. Furthermore, noise in the SLA field or temporary distortions of the shapes of the eddies contribute to the errors in the tracking phase.

The most evident weakness of our algorithm concerns the presence of gaps in the detected tracks. Occasionally, some eddies

Ocean Sci. Discuss., https://doi.org/10.5194/os-2017-93
Manuscript under review for journal Ocean Sci.
Discussion started: 15 January 2018

bump into other features or into meanders of the current, losing vorticity and becoming undetectable by the W-based algorithm. The tracking method is not able to recognise these gaps and attributes a new ID to the newly-formed eddy, which typically occurred a few days after the termination of another one, in the same position. As a result, the lifetime of the eddies could be incorrect and the tracks could be fragmented as well.

In order to solve this problem, we performed some improvements to the tracking methods by applying an eddy-continuity routine. For each vanishing eddy, the eddy-continuity algorithm examines all the structures which form in the following 7 days and computes the spatial distance and the difference in EKE between the new eddies and the vanished structure. If the distance is less than 50 Km (mean eddy radius in the study area) and simultaneously if the difference in energy is less than the 30% of the final EKE of the vanishing eddy, the algorithm joins the two structures, assigning to them the same ID. These threshold values are the results of sensitivity tests, obtained by the comparison of the tracks with the maps of SLA.

To assess the strength of the eddy-continuity routine, we compared its output with the main parameters of a mesoscale eddy described in literature on the basis of in situ and satellite data. Figure 2 shows all the eddies of the domain on four different days. We focus on the eddy with coordinates $3.8°$ E and $38.3°$ N, described by Cotroneo et al. (2016), who indicates the formation of the eddy in June, 2014, as supported by the application of the tracking methods of Mason et al. (2014). The black dots indicate the W contours and thus the structures detected by the algorithm. Until August 23^{rd}, 2014 (top-left), the algorithm detected the eddy born on June 13^{rd}. On August 24^{th} (top-right), the structure has interacted with another stronger eddy and lost vorticity. In the following 6 days the algorithm did not find any structure in that position. Thanks to the checking routine, we found the re-formation of the same eddy 7 days later, on August 30^{th} (bottom-left). The same occurred after a few day, with a jump of 3 days. After the second re-formation the eddy became stronger in vorticity, amplitude and EKE, moved north-westward, distancing the eastern stronger structure (bottom-right). From here on out the detection algorithm did not lose the trace of the eddy. Our dataset terminates on December 31^{st}, 2014, with the eddy still present in the basin. Figure 3 shows the tracks of the eddy before (Panel A) and after (Panel B) the application of the eddy-continuity algorithm. The red line indicates the correction to the original track. In the first case the results suggest a lifetime of 72 days, while after the correction the lifetime is over 202 days.

2.6 Methods limitations

The main advantage of the methods described in the previous sections (both physical and hybrid) is that they are automated and allow a large amount of data to be taken into consideration. Several years of satellite altimetry observations are thus used to investigate the mesoscale eddy seasonal and inter-annual variability. However, all methods mentioned above, when applied to altimetry data, take into account only the geostrophic velocities, while during their formation/vanishing phases the eddies are also subject to the ageostrophic components of velocity. Nevertheless, in order to track the eddies, the ageostrophic components are considered as negligible.

The EKE of each eddy has been computed using the geostrophic velocities anomaly *u* and *v*. Thus, the energy extrapolated from altimetry only describes geostrophic speed, whereas the "total kinetic energy" should include the ageostrophic components too and it is known that altimetry data can underestimate EKE by about half of its actual value (Pujol and Larnicol, 2005). However,

Ocean Sci. Discuss., https://doi.org/10.5194/os-2017-93
Manuscript under review for journal Ocean Sci.
Discussion started: 15 January 2018

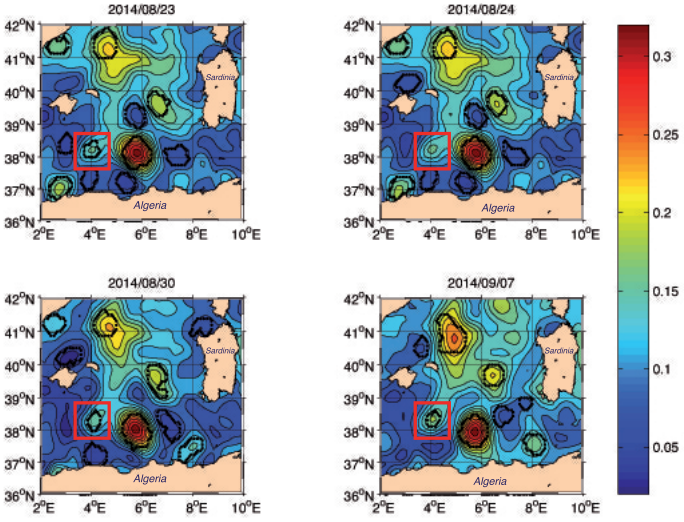

Figure 2. Maps of SLA of the domain on four different days (m). The black dots indicate the W contour and thus the structures detected by the algorithm. The figure shows a gap in the detection of the mesoscale structures.

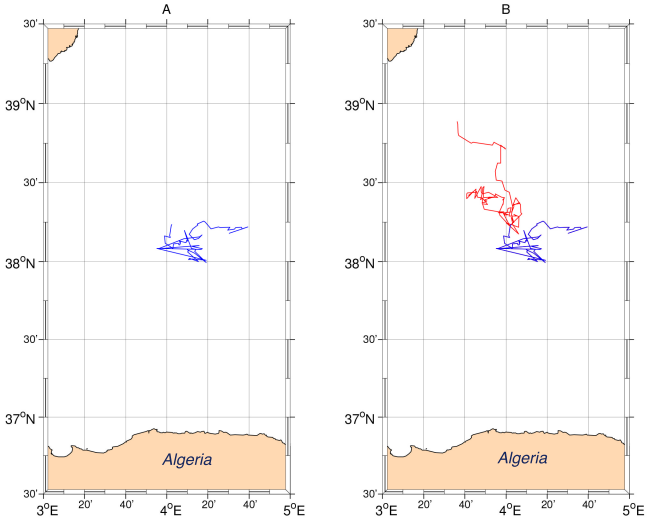

Figure 3. Tracks of the eddy described by Cotroneo et al. (2016) before/after the application of the eddy-continuity routine

in the study of the mesoscale circulation, the use of such data produces acceptable results.

Another issue with automated detection algorithms is the practical difficulty in defining an eddy boundary. Since eddies are fluid structures, time-dependent and continuously evolving without persistence, it is difficult to clearly demarcate their boundaries. There is some arbitrariness both in the definition of mesoscale eddies and in the method selected to define their borders (Chelton et al., 2011).

In some case identification of the geometry and of the boundaries can be further complicated as small eddies arise from the bifurcation of a bigger structure, as happens to the eddy described by Cotroneo et al. (2016).

Every method based on the calculation of the W parameter requires a threshold value, which is critical in the identification of the eddies. There is no single optimal value for the global ocean and too high or too low a value can fail to detect small features or overestimate the size of the eddy. In the latter case, the eddies with an unrealistic area may encompass multiple vortices, sometimes with opposite polarities. In order to avoid this problem, by using the hybrid method, we first detect the closed loop of SLA around the extrema and then, within the SLA loop, the closed loop of W.

Another problem of the physical methods is that the numerical computation of W is subject to noise in the SLA fields. In fact, the calculation of the second derivative of SLA fields amplifies the error (Chelton et al., 2011; Kurian et al., 2011). The application of the Hanning filter notably reduces the noise, but at the same time weakens the signal of some structures, making them difficult to be detected by the algorithm. The problem is solved by the application of the eddy-continuity routine, which fills the gaps in the tracks. It is also important to set a maximum radius to avoid mistakes in the eddy detection.

The association of regions of negative W and regions embedded in SLA closed loops avoids the detection of spurious features due to noise and removes the ambiguities in multi-poles/elongated closed loops (Halo et al., 2014). Furthermore, structures with lifetime shorter than 7 days are not considered in the analysis.

3 Results

Figure 4 shows the number of the eddy centres from 1993 to 2014 resampled in cells of $1/5^\circ$ x $1/5^\circ$. Such distribution is quite homogeneous, except for three areas, two in the southern part and one along the transect from Majorca Island to the Sardinian west coast where we observe a high concentration of eddy centres. In the Sardinia Channel (38° N, 8° E), known in literature as an eddy formation area (Escudier et al., 2016), we found the highest number of centres (up to 250 per sampling unit). At the same latitude, at about 6° E, we detect a second maximum (up to 180 centres). The third maximum is located in the northern region of the basin, at about 40° N, corresponding to the path of the WMMC, in proximity of the NBF.

It is important to underline that south-west of the Sardinian slope, close to the coast, we found less than 50 eddy centres. This area is characterised by upwelling phenomena (Olita et al., 2013) and by a quasi-permanent cyclonic circulation: the Southerly Sardinia Current (SSC) (Pinardi et al., 2013).

Figure 5 shows the averaged relative vorticity, normalised with respect to the Coriolis parameter (f), ξ/f, for all the anticyclonic structures detected over the full period. It ranges from 0.06 in absolute value in the northern basin up to 0.2 in

Ocean Sci. Discuss., https://doi.org/10.5194/os-2017-93
Manuscript under review for journal Ocean Sci.
Discussion started: 15 January 2018

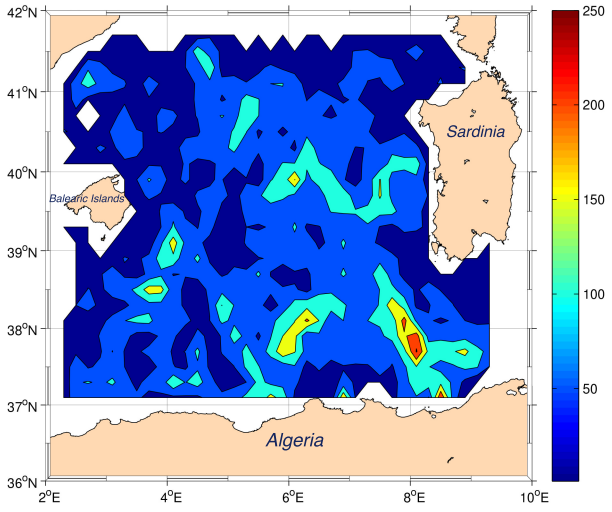

Figure 4. Contour plot of the number of the eddy centres from January 1993 to December 2014 with a grid resolution of $1/5^{\circ}$. The highest density is in proximity of the Sardinia Channel

the southern basin, along the Algerian Current. The area where we found the maximum number of centres, south of 39° N, corresponds to the area with higher values of vorticity, as it would be expected.

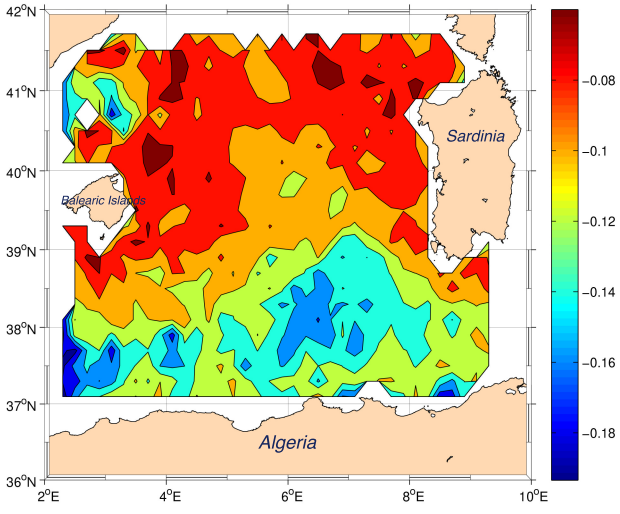

Figure 5. Contour plot of the mean relative vorticity normalised with respect to the Coriolis parameter (f), ξ/f, of the structures from January, 1993 to December, 2014, with a grid resolution of $1/5^{\circ}$. The largest (negative) values are in the southern basin, south of 39° N

The distribution of the averaged radii and amplitudes present a zonation similar to the above seen variables (not shown, while just EKE is shown in Figure 15).

Ocean Sci. Discuss., https://doi.org/10.5194/os-2017-93
Manuscript under review for journal Ocean Sci.
Discussion started: 15 January 2018

The distributions in Figures 4 and 5 suggest that the basin can be divided into two sub areas, north of and south of 39° N. Figure 6 shows the time series of monthly mean EKE (9) of the eddies from 39° N to 42° N and of the eddies from 37° N to 39° N . In particular, we computed the monthly mean of the daily energy of each centre. The values for the northern part fall in the range from 50 to 100 cm^2/s^2 with peaks up to 180 cm^2/s^2 in the years 1999, 2006 and 2011. The energy of the southern part shows the highest inter-annual variability with values about two or three times greater than the northern. The mean is centred on 200 cm^2/s^2 with peaks greater than 250 cm^2/s^2. The first peak, centred in 1997, has been detected also from Pujol and Larnicol (2005). The other peaks have been found in the periods November, 2004 - August, 2006, May, 2008 - May, 2010 and December, 2012 - December, 2014. All of them have a duration greater than one year.

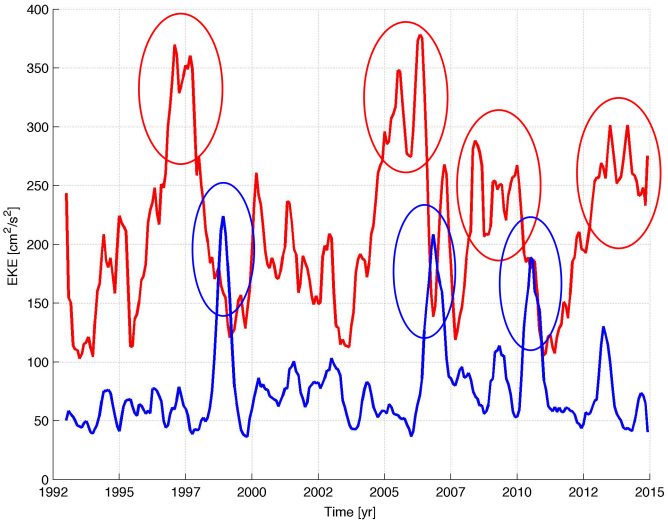

Figure 6. Time series of the monthly mean EKE (mmEKE) from 1993 to 2014. The mmEKE of the southern Algerian basin (37°-39° N) in red and of the northern basin (39°-42° N) in blue. The circles highlight the maximum values.

To evaluate the relationship between the lifetime and the properties of the eddies we calculated the mean kinetic energy (MEKE) and the mean radius of all the eddies with lifetime within a specific temporal range. The lifetime has been divided into 9 steps, of approximately 30 days each, from 7 to 240 and for lifetime greater than 8 months. Figure 7 - Panel A shows the averaged values and the standard deviation of the MEKE of the eddies for each lifetime step. The structures with lifetime up to 30 days have on average MEKE of 80 cm^2/s^2, while the eddies with a lifetime greater than 240 days reach MEKE of 400 cm^2/s^2. The relationship increases almost monotonically with high standard deviation.

The same study has been conducted for the mean radius of each eddy (Figure 7 - Panel B). Similarly, the structures with a short lifetime have a small radius (on average 30 Km for the first step). The mean radius reaches values around 40 Km for eddies longer than 90 days. It increases for eddies longer than 240 days, reaching 47 Km.

Ocean Sci. Discuss., https://doi.org/10.5194/os-2017-93
Manuscript under review for journal Ocean Sci.
Discussion started: 15 January 2018

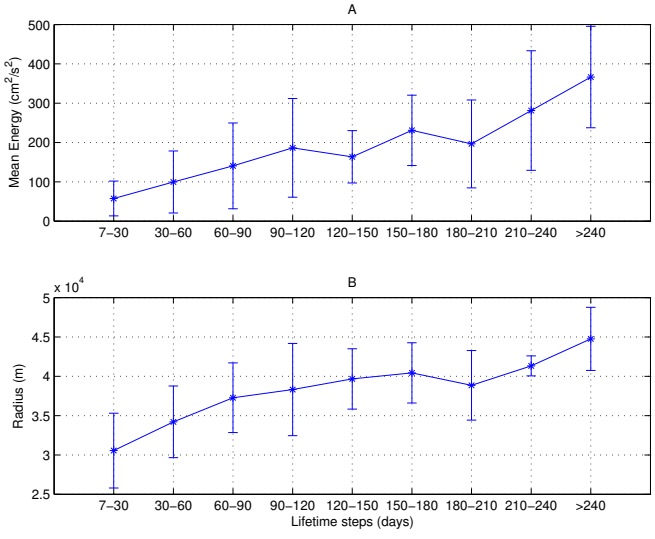

Figure 7. Relation between MEKE (A), radius (B) and lifetime. There are 9 lifetime steps 30 days long. Averages have been computed on the basis of MEKEs and mean radii of the eddies in the basin.

To identify the areas of formation, convergence, detaching and vanishing of the eddies we superimposed a regular grid on the domain. The 6 sectors are labelled from A to F (Figure 9). Each is $2°$ of latitude and $2°$ of longitude, from $2.5°$ E to $8.5°$ E and from $37°$ N to $41°$ N. We posit that they have different pathways and lifetime depending on their area of formation and kinetic energy.

Short-life anticyclonic eddies (shorter than 90 days)

In Figure 8, the histograms show the number of short-life eddies formed (blue bars), vanished (green bars) and both formed and vanished in each sector (yellow bars). The difference between the yellow and the green bars represents the number of eddies coming from other parts of the basin and vanishing in a given sector. It could be an indirect indication for zone of convergence. The higher number of formations is concentrated in sector B (280 eddies), and more generally the northern part of the basin (A-C) hosts more formations of short-life eddies (713) than the 510 of southern part (D-F). Furthermore, the yellow bars show that almost all the eddies formed in each of the six sectors vanished in their sector of formation. In the northern sectors the percentage exceeds the 80%, while it is reduced in the southern sectors (72.8% in D, 80.8% in E and 77.4% in F).
Figure 9 shows the tracks of the eddies formed in sectors B, D and F because they are the areas with the most eddy formation respectively at the northern and southern parts of the basin. Short-life eddies do not move around the basin, but rather they remain close to their area of formation. In fact, despite their mean translational velocity of $4\ Km/day$ and an average lifetime of $30 - 40$ days, they tend to follow a random pathway and do not move far from where they originated. In general, just a few eddies, usually the more energetic ones, move to another sector. Some of the structures formed in D follow the pathway of the

Ocean Sci. Discuss., https://doi.org/10.5194/os-2017-93
Manuscript under review for journal Ocean Sci.
Discussion started: 15 January 2018

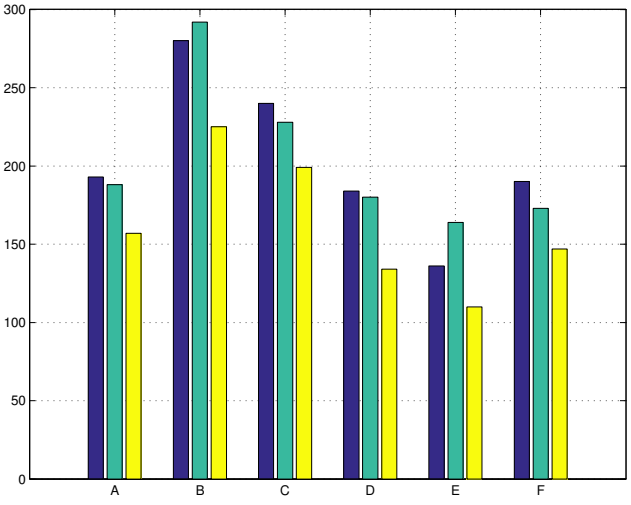

Figure 8. Number of short-life eddies formed in each sector (blue), formed and terminated in the same sector (yellow) and terminated in each sector (green). Sectors A, B and C are located in the northern part of the basin, while D, E and F are in the southern part.

AC and move along the coast, till sector E. In all the sectors the distribution of the eddy formation is homogeneous. Almost all the structures born in sector F do not pass across the Sardinia Channel but vanish west of 9° E. Just the 3% of the eddies born east of 8° E can pass through the strait and vanish east of 9° E.

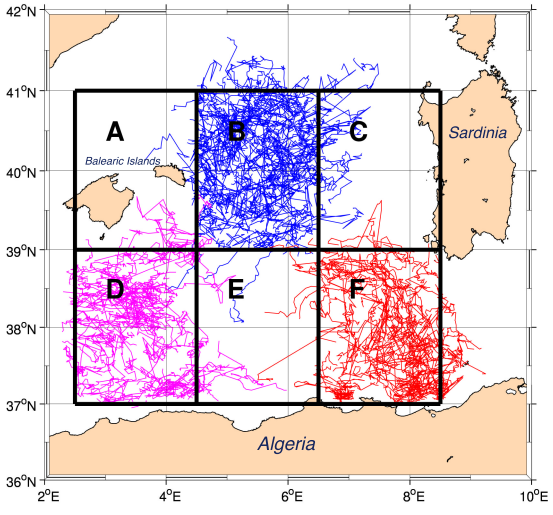

Figure 9. Tracks of the short-life eddies formed in sectors B (blue), D (magenta) and F (red).

The structures formed in the areas A, B and C do not cross 39° N, except for a few cases. These structures have been detected in the past by Fuda et al. (2000), who labelled them Frontal Algerian Eddies (FAEs), considering only structure with lifetime

Ocean Sci. Discuss., https://doi.org/10.5194/os-2017-93
Manuscript under review for journal Ocean Sci.
Discussion started: 15 January 2018

up to 15 days. We use the name FAEs to indicate short- or long-life eddies, formed along the NBF. We hypothesize they are caused by the instabilities of the NBF.

Thanks to the availability of a large amount of data, it has been possible to evaluate the seasonal variability of the formation of the eddies in the basin. Figure 10 shows a homogeneous distribution of formation of short-life eddies during the year, with two peaks in fall and winter, i.e. from October to March, when formation number is more than 450.

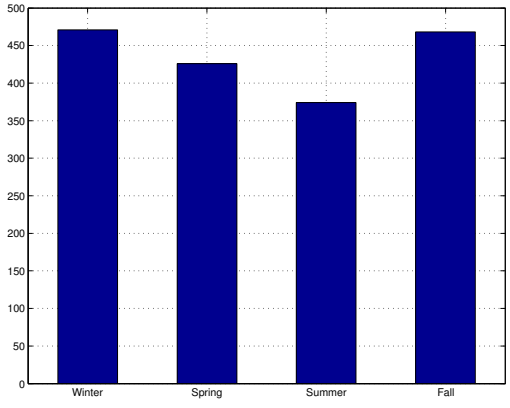

Figure 10. Figure shows the number of formations of short-life eddies in each season for the period 1993 to 2014. Winter includes the months from January to March, spring from April to June, summer from July to September and fall from October to December.

Long-life anticyclonic eddies

The same analyses have been performed for eddies with lifetime greater than 90 days (Figure 11). The biggest number of long-life eddies formation centres is in the Sardinia Channel, between 6.5° E and 8.5° E (sector F, 26 eddies). The AEs move cyclonically around the basin, typically with their centre remaining south of 39° N, sometimes completing an entire loop (Figure 12, Panel A). They often vanish in sector E, where we found the biggest number of deaths (56.5%). 54% of the FAEs follow the same cyclonic loop as well (Figure 12, Panel B). In sector E the difference between the number of terminations of eddies coming from other areas and eddies born there is very high (24) and the same occurs also for the short-life structures. It suggests the area to be a convergence zone for the eddies, as highlighted by the large number of centres (Figure 4).

It is important to underline that all the long-life eddies formed in sector F do not pass the Sardinia Channel, but deviate northwards and follow a cyclonic loop.

The number of formations is maximum in spring (26 formations, almost $2-3$ times the number of formations in the other seasons - Figure 13) when the maximum transport through the Strait of Gibraltar occurs (Beranger et al., 2005).

The seasonality of the long-life structures is thus reversed respect to the short-life.

Ocean Sci. Discuss., https://doi.org/10.5194/os-2017-93
Manuscript under review for journal Ocean Sci.
Discussion started: 15 January 2018

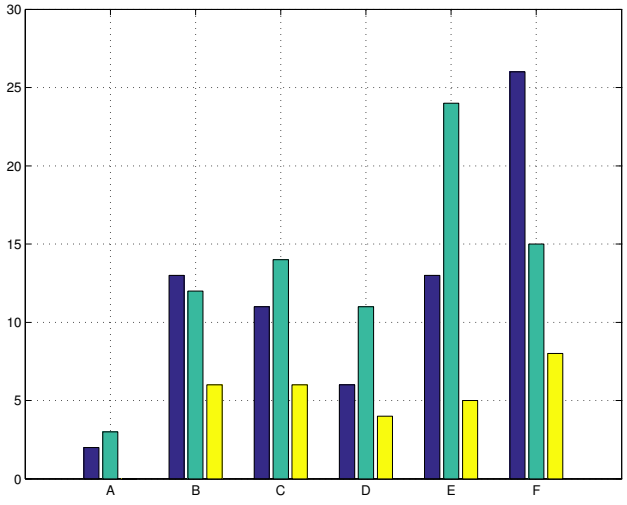

Figure 11. Number of long-life eddies formed in each sector (blue bars), formed and terminated in the same sector (yellow bars) and terminated in each sector (green bars). Sectors A, B and C are located in the northern part of the basin, sectors D, E and F in the southern part

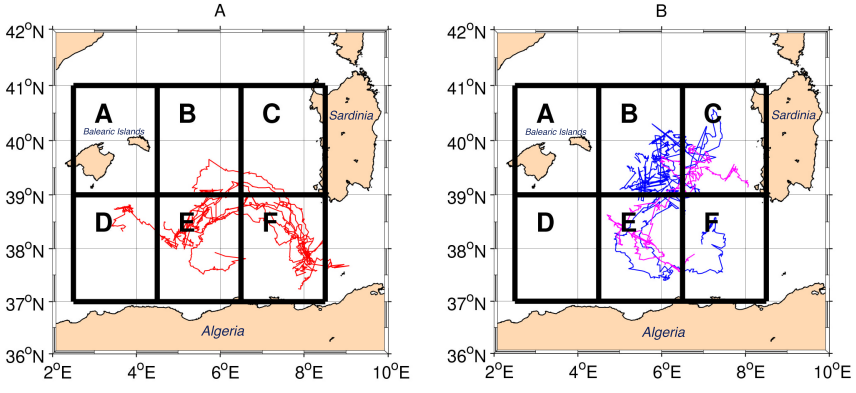

Figure 12. Tracks of long-life eddies born in sectors F (Panel A) and in sectors B and C (Panel B).

Ocean Sci. Discuss., https://doi.org/10.5194/os-2017-93
Manuscript under review for journal Ocean Sci.
Discussion started: 15 January 2018

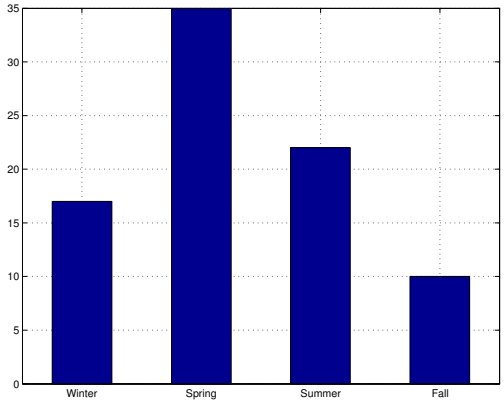

Figure 13. Figure shows the number of formations of long-life eddies in each season from 1993 to 2014. Winter includes the months from January to March, spring from April to June, summer from July to September and fall from October to December.

Long-life eddies and EKE peaks

Figure 6 shows four energy peaks longer than one year, while Figure 7 suggests the long-life eddies to be the most energetic structures. In order to verify that the four peaks actually correspond to the presence of long-life eddies within the basin, we analysed the tracks of structures with lifespan greater than 450 days. We found 5 features (Figure 14) in years $1995-1997$ (Panel A), $2004-2007$ (Panel B), $2009-2010$ (Panel C) and $2012-2014$ (Panel D).

The first peak in Figure 6, corresponding to the highest values of mmEKE, is related to the longest track which starts on December, 25^{th}, 1995 and terminates on November 19^{th}, 1997 (Panel A). It is the well-known long-life structure $96/1$ studied by Puillat et al. (2002). The second high peak, in the period from 2004 to 2007, is associated with two long-life eddies (Panel B), while the lower peak corresponds to the shorter track (Panel C).

As suggested by previous analyses, all the long-life eddies spend the most of their life south of $39°$ N, except for two structures which terminate in the northern basin. The area where the features can cross $39°$ N is in the middle of the basin (between $5°$ E and $7°$ E) and is characterised by large (negative) mean relative vorticity (Figure 5).

Eddy translational velocity

In order to find the main translation direction of the eddies, we divided the basin with a regular grid of $\frac{1}{5}^{\circ}$ and we computed the average values of the components u and v of the translational velocity (Figure 15). The mean translational speed of the eddies in the basin is 5.7 cm/s. The map confirms that on average the eddies follow the AC till $8°$ E. In proximity of the Sardinia Channel they deviate northward entering in a cyclonic loop, south of $39°$ N. The highest speeds (up to 9 cm/s) are reached along the AC and where the eddies detach from the coast and move offshore. The cyclonic loop is also characterized by high speeds, while lower speeds are found in the middle of the basin, where eddies interact with the AC and other structures and where we found the highest kinetic energy (up to $360\ cm^2/s^2$). Furthermore, this area hosts a large number of centres (Figure

Ocean Sci. Discuss., https://doi.org/10.5194/os-2017-93
Manuscript under review for journal Ocean Sci.
Discussion started: 15 January 2018

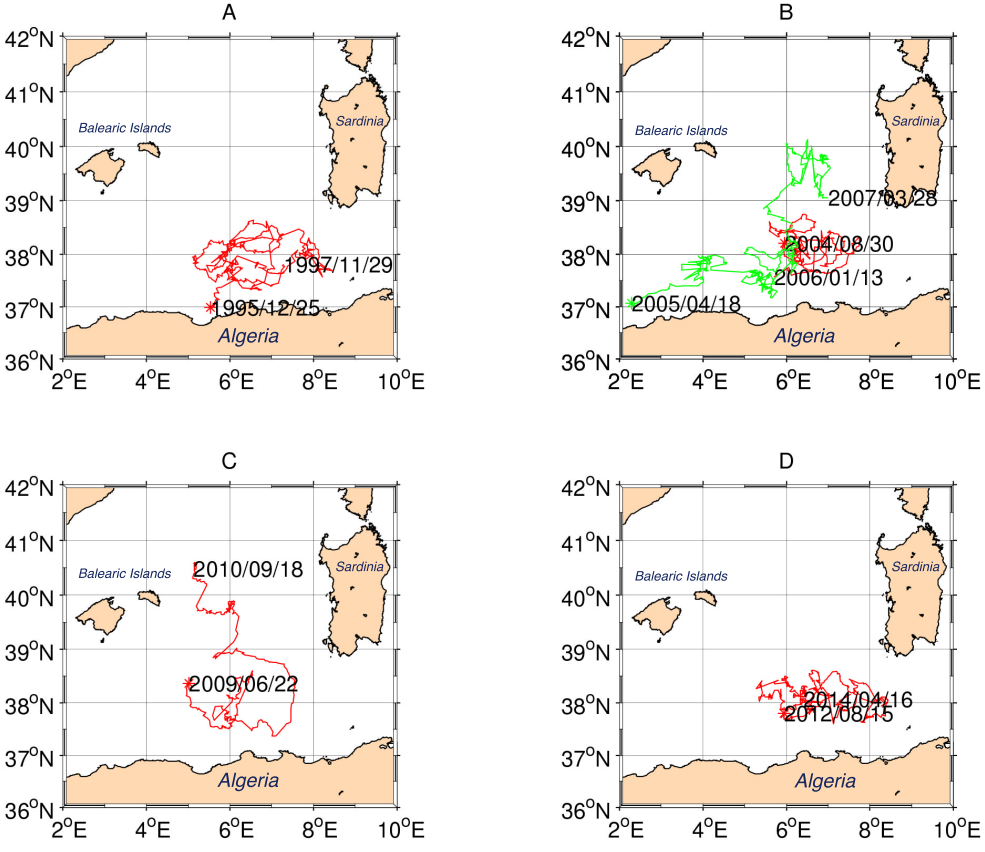

Figure 14. Tracks of structures with lifespan greater than 450 days. The dates indicate the formation and the termination of each eddy.

4), and a maximum of (negative) relative vorticity (Figure 5). It makes the region of particular interest from the dynamical point of view.

In the northern part of the basin, north of 39° N, the mean translational velocities are less than in the southern part and do not present a predominant direction.

4 Summary and conclusions

The automated method for eddy detection and tracking, applied over 22 years of merged altimetry SLA maps, allows us to characterise the variability of mesoscale structures and, in general, describe mesoscale circulation, which is strongly influenced by the pathways of the eddies within the basin.

As mentioned in Section 2, the hybrid method presents a number of advantages reducing the disadvantages of other methods. It is important to note that the tracking method is based on the definition of a general distance (15), which in turn defines the evolution of each eddy over time. In a basin as small as the Algerian Basin, eddies frequently encounter other eddies and

Ocean Sci. Discuss., https://doi.org/10.5194/os-2017-93
Manuscript under review for journal Ocean Sci.
Discussion started: 15 January 2018

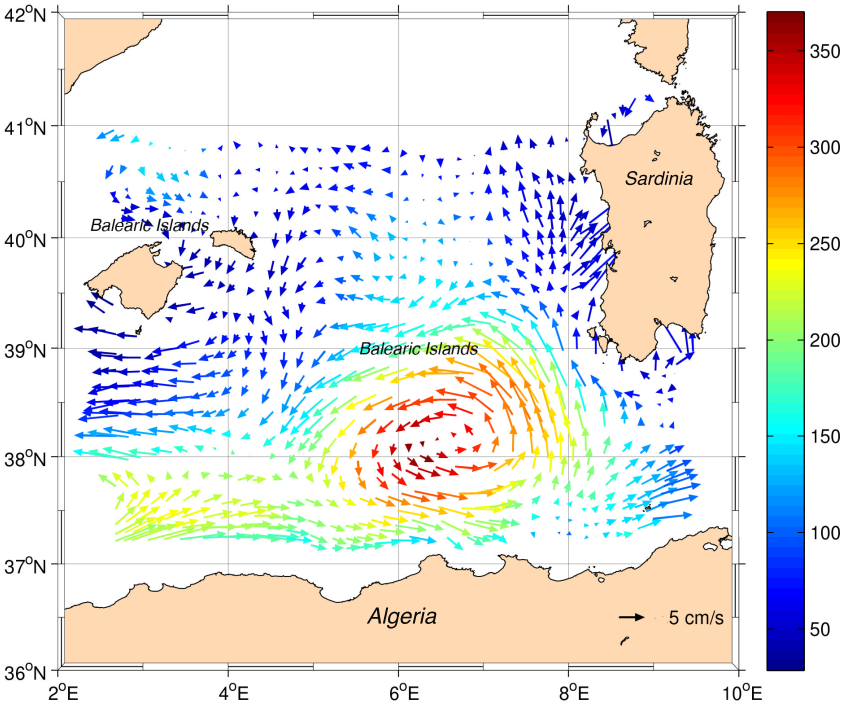

Figure 15. Average velocities in cm/s of the eddies in boxes of $\frac{1}{5}^{\circ}$. The colour indicates the average daily EKEs (cm^2/s^2) in the same boxes

deviate from their paths or merge into new, larger structures (coalescence). A significant limitation of the algorithm is its inability to recognise weak signals in the eddy vorticity (causing gaps in the continuous tracking, here called *jumps*), and as a consequence, the mis-identification of old eddies as new ones. This limitation affects both the definition of a pathway and the estimate of their lifetime and number. To overcome this limitation, we implemented an eddy-continuity routine, which detects if, in the 7 days following a death, a new eddy arises with close values of EKE and in a close position. The comparison with existing literature (Puillat et al., 2002; Escudier et al., 2016; Cotroneo et al., 2016) and some sensitivity tests (not shown) have demonstrated the reliability of the detection/tracking algorithm and the improvement given by the implementation of the eddy-continuity routine.

After estimating their duration, we decided to ignore eddies with lifetime shorter than 7 days, as the algorithm may introduce spurious short-lived structures. We performed a eulerian statistic on eddies shorter and longer than 90 days separately, in order to study their spatial distribution. We found that the short-life eddies mostly form in the northern part of the basin (58% north of 39° N) and are less energetic. They barely move within the basin and terminate close to their area of formation. The remaining 42% short-life eddies, mostly found south of 39° N, have higher kinetic energy.

This result complements that of long-life eddies, which typically form south of 39° N (63%). The area of formation is located from 6.5° E and 8.5° E, in proximity to the Sardinia Channel. Long-life eddies probably absorb energy from the Algerian Current and move cyclonically within the basin, without straying north of 39° N. Sector F can be considered not only a formation

Ocean Sci. Discuss., https://doi.org/10.5194/os-2017-93
Manuscript under review for journal Ocean Sci.
Discussion started: 15 January 2018

zone, but also a detaching area, where coastal eddies become open-sea eddies. The remaining 37% long-life eddies form north of $39°$ N (sectors A-C). The most energetic ones move southward and join the cyclonic loop.

Due to the low persistence of short-life eddies in the basin, we suppose that they do not influence the physical, chemical and biological properties of the WMED.

We detected an area of convergence corresponding to sector E, from $4.5°$ E to $6.5°$. Long-life features forming in sector F or coming from the northern basin (sectors B and C) terminate there. Also, some of the short-life AEs formed in sector D following the Algerian Current die in sector E, as do some short-life structures coming from sector B. These eddies are known in literature not to become open sea eddies (Obaton et al., 2000; Millot et al., 1997). In this area the Algerian Current spreads seaward for months (Benzhora and Millot, 1995b; Millot et al., 1997).

The monthly mean kinetic energy of the structures shows a clear separation between the northern and the southern part of the basin. The latter is about three times more energetic than the former (up to $300\ cm^2/s^2$) and is subject to annual periodicity (not shown). This is in accordance with the study of Pujol and Larnicol (2005) which also highlights that the seasonal EKE variations are mainly concentrated southwest of Sardinia. The four peaks of energy in the northern basin correspond to the eddies with lifetime greater than 450 days. It confirms the proportionality between lifetime and eddy kinetic energy. The maximum centred in the year 1997 is also present in the EKE computed at the basin scale by Pujol and Larnicol (2005).

By examining the properties of each eddy, we found that the longer the lifetime of the structures, the larger their radius and the higher their kinetic energy.

In literature, southern eddies formed along the Algerian Current are commonly referred to as Algerian Eddies (AEs). In order to distinguish the eddies formed in the two parts of the basin, we labelled the northern structures (both short- and long- life) Frontal Anticyclonic Eddies (FAEs) (Fuda et al., 2000), as we suppose that they are caused by the instabilities of the NBF. Northern and southern structures differ on the basis of lifetime, pathway and other properties such as energy and dimension.

The complementarity between short- and long-life structures has also been observed in the study of seasonality. Short-life eddies form mostly in autumn and winter, while long-life eddies typically form in spring in the southern basin, when the AC is at its maximum transport (Beranger et al., 2005). It was observed that the transport through the Strait is the physical parameter which supports the eddy formation mechanism (Obaton et al., 2000). The density gradient becomes stronger, facilitating baroclinic instabilities.

The cyclonic loop of the eddies in the southern part of the basin corresponds to the high-energy and high-density pathways and is partly superimposed on the Algerian Gyre, flowing in the LIW layer (Testor et al., 2005b; Escudier et al., 2016). The along-slope propagation of southern AEs stops in proximity to the Sardinia Channel, where the structures probably interact with the bathymetry and with a salinity (and density) barrier, which may contribute to blocking the propagation of eddies. We suppose the structures remain there until they absorb from the Algerian Current an amount of energy sufficient to detach from the coast and move northward.

The Algerian Basin can be considered as consisting of two areas: the northern one is characterized by eddies with shorter lifespan and smaller values of EKE, relative vorticity and translational velocity. There is no connection between the two areas, except for the (Frontal Eddies) FAEs, which deviate southward and join the cyclonic loop, in correspondence with the Algerian

Gyre's pathway, as highlighted by high values of mean velocities and kinetic energy.

The area between $4.5°$ and $6.5°$ E, along the Algerian coast, is known in literature (Escudier et al., 2016) as a formation zone for mesoscale eddies. Contrary to the current body of research, we observed the formation of just a handful of eddies and numerous terminations. By observing the tracks, we found that a large number of eddies originating from other sectors pass here. Thus, we argue that this area could be a convergence zone for the mesoscale eddies within the Algerian Basin. The presence of a large number of structures can constitute a block for the Algerian Current, which sometimes presents big meanders that move seaward. It is well highlighted by satellite imagery and Mean Dynamic Topography data (not shown).

In the past, some of the AEs were supposed to pass the Sardinia Channel and continue their motion along the coast. Several satellite images show consecutive vortices through the Sardinia Channel and in the south of the Tyrrhenian Sea. We observed that some of the short-life AEs formed in the south-eastern part of the basin pass through the Sardinia Channel and die immediately after the channel (before $9°$ E). They could be blocked also by the quasi-permanent cyclonic circulation, associated to the upwelling phenomena, south-east of Sardinia. Based on the results of our work on the trajectories of the AEs, we hypothesize that the eddies formed in the Algerian Basin recirculate there, without reaching the Tyrrhenian Sea. We suppose that the structures which can pass through the channel and flow to the Tyrrhenian Sea have formed after $10°$ E. These features are in proximity to the border of our domain and thus this topic will be object of a further study in the near future.

Acknowledgements. This paper is supported by the and co-financed by the European Regional Development Found, by Italian Flagship Project RITMARE founded by the Italian Ministry for Research – MIUR (NRP 2011-2013, approved by the CIPE Resolution 2/2011 of 23.03.2011).

Ocean Sci. Discuss., https://doi.org/10.5194/os-2017-93
Manuscript under review for journal Ocean Sci.
Discussion started: 15 January 2018

References

Aulicino, G., Cotroneo, Y., Ruiz, S., Sánchez Román, A., Pascual, A., Fusco, G., Tintoré, J., and Budillon, G.: Monitoring the Algerian Basin through glider observations, satellite altimetry and numerical simulations along a SARAL/AltiKa track, Journal of Marine Systems, 179, 55–71, 2018.

Benzhora, M. and Millot, C.: Hydrodynamics of an open sea Algerian Eddy, Deep Sea Research Part I: Oceanographic Research Papers, 42, 1831–1847, 1995a.

Benzhora, M. and Millot, C.: Characteristics and circulation of the surface and intermediate water masses of Algeria, Deep Sea Research Part I: Oceanographic Research Papers, 42, 1803–1830, 1995b.

Beranger, K., Mortier, L., and Crepon, M.: Seasonal variability of water transport through the Straits of Gibraltar, Sicily and Corsica, derived from a high-resolution model of the Mediterranean circulation, Ocean Science, 66, 341–364, 2005.

Budillon, G., Cotroneo, Y., Fusco, G., and Rivaro, P.: Variability of the Mediterranean Deep and Bottom Waters: Some Recent Evidences in the Western Basin, CIESM Workshop Monographs, 2009.

Burkov, V., Krivosheya, V., Ovchinnikov, I., and Savin, M.: Eddies in the current system of the Western Mediterranean Sea, Oceanology, 19, 9–13, 1979.

Chaigneau, A., Eldin, G., and Dewitte, B.: Eddy activityin the four major upwelling systems from satellite altimetry (1992-2007), Progress in Oceanography, pp. 117–123, 2009.

Chelton, D. B., Schlax, M. G., Samelson, R. M., and De Szoeke, R. A.: Global observations of large oceanic eddies, Geophys. Res Lett., 2007.

Chelton, D. B., Schlax, M. G., and Samelson, R. M.: Global observations of nonlinear mesoscale eddies, Progress in Oceanography, pp. 167–216, 2011.

Cotroneo, Y., Aulicino, G., Ruiz, S., Pascual, A., Budillon, G., Fusco, G., and Tintoré, J.: Glider and satellite high resolution monitoring of a mesoscale eddy in the algerian basin: Effects on the mixed layer depth and biochemistry, Journal of marine systems., 162, 73–88, 2016.

Escudier, R., Mourre, B., Juza, M., and Tintoré, J.: Sub-surface circulation and mesoscale variability in the Algerian sub-basin from altimeter-derived eddy trajectories, Journal of Geophysical Research: Oceans, 2016.

Font, J., Millot, C., Salas, J., Julià, A., and O.Chic: The drift of Modified Atlantic Water from the Alboran Sea to the eastern Mediterranean, Scientia Marina, pp. 211–216, 1998.

Font, J., Isern-Fontanet, J., and Salas, J.: Tracking a big anticyclonic eddy in the Western Mediterranean Sea, Scientia Marina, pp. 331–342, 2004.

Fuda, J. L., Millot, C., Taupier-Letage, I., Send, U., and Bocognano, J. M.: XBT monitoring of a meridian section across the Western Mediterranean Sea, Deep-Sea Research I, pp. 2191–2218, 2000.

Fusco, G., Artale, V., Cotroneo, Y., and Sannino, G.: Thermohaline variability of Mediterranean Water in the Gulf of Cádiz, 1948–1999, Deep-Sea Res I, 55, 1624–1638, 2008.

Halo, I., Backeberg, B., Penven, P., Ansorge, I., Reason, C., and Ullgren, J. E.: Eddy properties in the Mozambique Channel: A comparison between observations and two numerical ocean circulation models, Deep-Sea Research, II, 38–53, 2014.

Isern-Fontanet, J. and E. Garcìa-Ladona, J. F.: Identification of marine eddies from altimetry, J. Atmos. Ocean. Tech, pp. 772–778, 2003.

Isern-Fontanet, J., Garcia-Ladona, E., and Font, J.: Vortices of the Mediterranean Sea: an altimetric perspective, Journal of physical oceanography, 36, 87–103, 2005.

Jeong, J. and Hussain, F.: On the identification of a vortex, Journal of Fluid Mechanics, pp. 69–94, 1995.

Kurian, J., Colas, F., Capet, X., McWilliams, J. C., and Chelton, D. B.: Eddy properties in the California Current System, Journal of Geophysical Research, 2011.

Levy, M., Memery, L., and Madec, G.: The onset of the spring bloom in the MEDOC area: mesoscale spatial variability, Deep-Sea Res I, pp. 1137–1160, 1999.

Levy, M., Memery, L., and Madec, G.: Combined effects of mesoscale processes and atmospheric high-frequency variability on the spring bloom in the MEDOC area, Deep-Sea Res I, pp. 27–53, 2000.

Mason, E. and Pascual, A.: Multiscale variability in the Balearic Sea: An altimetric perspective, Journal of Geophysical Research: Ocean, 118, 1–19, 2013.

Mason, E., Pascual, A., and McWilliams, J.: A new sea surface height based code for mesoscale oceanic eddy tracking, J. Atmos. Oceanic Technol., 31, 1181–1188, 2014.

McWilliams, J. C.: The vortices of homogeneous geostrophic turbulence, Journal of Fluid Mech., pp. 1–26, 1999.

Millot, C.: Some features of the Algerian Current, Journal of Geophysical Research: Oceans, 90, 7169–7176, doi: 10.1029/JC090iC04p07169, 1985.

Millot, C.: Circulation in the Western Mediterranean Sea, Oceanol. Acta, pp. 143–149, 1987.

Millot, C.: Circulation in the Western Mediterranean Sea, J Mar Syst, pp. 423–442, 1999.

Millot, C., Benzohra, M., and Taupier-Letage, I.: Circulation in the Algerian Basin inferred from the MEDIPROD-5 current meters data, Deep Sea Res, pp. 1467–1495, 1997.

Moràn, X. A. G., I-Taupier-Letage, Vazquez-Dominguez, E., Ruiz, S., Arin, L., Raimbault, P., and Estrada, M.: Physical-biological coupling in the Algerian Basin (sw mediterranean): influence of mesoscale instabilities on the biomass and production of phytoplankton and bacterioplankton, Deep Sea Research Part I: Oceanographic Research Papaers, 48(2), 405–437, 2001.

Obaton, D., Millot, C., d'Hières, G. C., and Taupier-Letage, I.: The Algerian Current: comparison between in situ and laboratory data sets, Deep-Sea Res., pp. 2159–2190, 2000.

Olita, A., Ribotti, A., Sorgente, R., Fazioli, L., and Perilli, A.: SLA-chlorophyll-a variability and covariability in the Algero-Provençal Basin (1197-2007) through combined use of EOF and wavelet analysis of satellite data, Ocean Dynamics (2011), pp. 89–102, 2011.

Olita, A., Ribotti, A., Fazioli, L., Perilli, A., and Sorgente, R.: Surface circulation and upwelling in the Sardinia sea: a numerical study, Continental Shelf Research, pp. 95–108, 2013.

Olita, A., Sparnocchia, S., Cusì, S., Fazioli, L., Sorgente, R., Tintoré, J., and Ribotti, A.: Observations of a phytoplankton spring bloom onset triggered by a density front in NW Mediterranean, Ocean Science, 10, 657–666, 2014.

Pasquero, C. and A. Provenzale, A. B.: Parametrization of dispersion in two dimensional turbulence, Journal of Fluid Mechanics, pp. 279–303, 2001.

Penven, P. and Echevin, V.: Average circulation, seasonal cycle, and mesoscale dynamics of the Peru Current System: A modeling approach, Journal of Geophysical Research, 2005.

Pinardi, N., Zavatarelli, M., Adani, M., Coppini, G., Fratianni, C., Oddo, P., Simoncelli, S., Tonani, M., Lyubartsev, V., Dobricic, S., and Bonaduce, A.: Mediterranean Sea large-scale low-frequency ocean variability and water masses formation rates from 1987 to 2007: A retrospective analysis, Progress in Oceanography, 2013.

Puillat, I., Taupier-Letage, I., and Millot, C.: Algerian Eddies Lifetime can near 3 years, Journal of Marine Systems, pp. 245–259, 2002.

Pujol, M.-I. and Larnicol, G.: Mediterranea Sea eddy kinetic energy variability from 11 years of altimetric data, Journal of Marine Systems, 58, 121–142, 2005.

Rio, M.-H., Pascual, A., Poulain, P.-M., Menna, M., Barceló, B., and Tintoré, J.: Computation of a new mean dynamic topography for the Mediterranean Sea from model outputs, altimeter measurements and oceanographic in situ data, Ocean Science, 10, 731–744, 2014.

Ruiz, S., Pascual, A., Garau, B., Faugère, Y., Alvarez, A., and Tintoré, J.: Mesoscale dynamics of the Balearic Front, integrating glider, ship and satellite data, Journal of Marine Systems, pp. S3–S16, 2009.

Schütte, F., Brandt, P., and Karstensen, J.: Occurrence and characteristics of mesoscale eddies in the tropical northeastern Atlantic Ocean, Ocean Science, 12, 663–685, 2016.

Taupier-Letage, I., Puillat, I., Millot, C., and Raimbault, P.: Biological response to mesoscale eddies in the Algerian Basin, J. Geophys. Res, 2003.

Testor, P., Béranger, K., and Mortier, L.: Modeling the deep eddy field in the southwestern Mediterranean: The life cycle of Sardinian eddies, Geophisical Research Letters, 32, 2005a.

Testor, P., Send, U., Gascard, J., Millot, C., Taupier-Letage, I., and Béranger, K.: The mean circulation of the southwestern Mediterranean Sea: Algerian Gyres, Jurnal of Geophisical Research, 110, 2005b.

Vignudelli, S.: Potential use of ERS and Topex/Poseidon altimeters for resolving oceanographic patterns in the Algerian Basin, Geophys Res Lett, pp. 1787–1790, 1997.

Yi, J., Du, Y., He, Z., and Zhou, C.: Enhancing the accuracy of automatic eddy detection and the capability of recognizing the multi-core structures from maps of sea level anomaly, Ocean Science, 10, 39–48, 2014.